

Design Optimization and Efficiency Enhancement of Linear Induction Motor

Dr. Adil H. Ahmad

Electrical Engineering Department, University of Technology/Baghdad

Marwa Mohammad Marei

Electrical Engineering Department, University of Technology/Baghdad

Email: m.Scmm86@yahoo.com

Received on: 21/9/2010 & Accepted on: 3/3/2011

ABSTRACT

This paper presents the dynamic behavior of a Single Sided Linear Induction Motor (SLIM) by changing many design parameters of a reference model of SLIM then an optimization process is adopted to give the final equivalent circuit of the proposed modified model. This analysis is prepared by using MATLAB package, version 7.8 (R2009a) for optimization and enhancement evaluation. The improvement in performance is performed by enhancing the efficiency power factor product ($\eta \cos \varphi$) which can be regarded as the enhancement criteria for the modified model of this motor. This factor improved from 0.23 of the reference model to 0.66 of the optimized model.

امثلة التصميم وتحسين الكفاءة للمحرك الحثي الخطي

الخلاصة

يتناول البحث دراسة السلوك الديناميكي للمحرك الحثي الخطي أحادي الجانب وذلك بتغيير معالم التصميم الأساسية لهذا المحرك. كما تمت عملية اختيار عناصر الدائرة المكافئة باستخدام طريقة الأمثلية للحصول على نموذج مُعدّل وهو النموذج المقترح بالاعتماد على نموذج أساسي حيث تم ذلك باستخدام برنامج الـ MATLAB. تم اختيار حاصل ضرب الكفاءة و معامل القدرة ($\eta \cos \varphi$) كمعيار لبيان مقدار التحسين في الأداء للنموذج المقترح وتم زيادة هذا العامل من 0.23 إلى 0.66 للنموذج المحسن.

INTRODUCTION

Linear Induction Motor (LIM) is a non-conducting, high speed linear motor that operates on the same principle as a rotary squirrel cage induction motor. There are many types of LIM; it can be Single Sided LIM (SLIM), Double Sided LIM (DLIM) and Tubular LIM (TLIM). The single sided LIM can be obtained (imaginary process) by "cutting" a cylindrical induction motor along its radius from the center axis of the shaft to the external surface of the stator core and "Rolling" it out flat[1]. LIM consists of excitation element called the stator and induced current element called the rotor. The primary (stator) contains a

three phase winding and uniform slots of the laminated iron core. These winding produce linearly traveling magnetic field.

The secondary (rotor) is either Ferro or nonferrous sheet metal, with and without solid or laminated back iron, used to complete the magnetic circuit. Due to the primary traveling field, a secondary current induced in the reaction plate. The interaction between the induced current and the changing electromagnetic field will generate electromagnetic thrust on the plate where linear speed is produced. Since there is no any physical coupling between the primary and the secondary, a silent operation is produced with reduced maintenance [2].

A linear induction motors (LIMs) are widely used in machine tools, linear tables, textile tools, saws, separators, operation of sliding doors and many other applications because LIM can get direct linear motion and management of a device is easy [3].

Figure (1) shows the topology of single sided LIM.

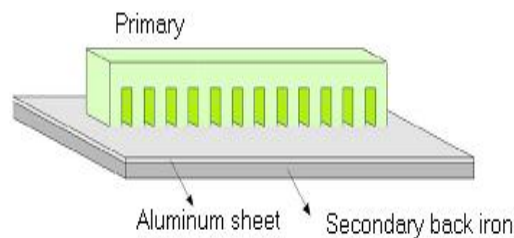


Figure (1) Topology of single sided LIM.

ANALYSIS TECHNIQUE FOR LIM

Design of LIMs has so far been presented based on different modelling techniques including magnetic equivalent circuit (MEC), layer model, and finite element method (FEM). MEC has some advantages over other methods for preliminary design of LIM which lie in its simplicity and suitability for optimization and this method is used in present paper [4].

Finite Element method (FEM)

The power and versatility of finite element method are well known, and have led to rapid growth in using it for solving electromagnetic field computation for electrical machine studies, where the whole machine model can be simulated and the performance can be computed. LIM analysis is performed by using finite element method FEM to simulate and study the geometry optimization of LIM using both two and 3-dimensional analysis [5]. In such analysis method, many results are obtained by using FEM analysis and using ANSYS program. These results contain magnetic vector potential, flux density, field intensity, magnetic forces, current density, and flux line distribution for both two and three dimensional analysis of linear induction motor.

Equivalent circuit method

The dynamic model of the linear induction motor (LIM) can be analyzed by using the d-q model of the equivalent electrical circuit with end effects included. The q-axis equivalent circuit of the LIM is identical to the q-axis equivalent circuit of the rotating induction motor (RIM). Where its parameters do not vary with the end effects.

However, in the d-axis equivalent circuit entry secondary currents affect the air gap flux. When the primary moves, the secondary is continuously replaced by a new material. This new material will tend to resist a sudden increase in flux penetration and only allow a gradual build up of flux density in the air-gap [6].

Both theory and experiment show that at the entry end, the normal component of the air magnetic flux density is weakened and at the exit end the normal component is amplified. Flux density distribution is shown in Figure (2) for $v_r=0$ and for v_r greater than zero as shown in Figure (3) [7].

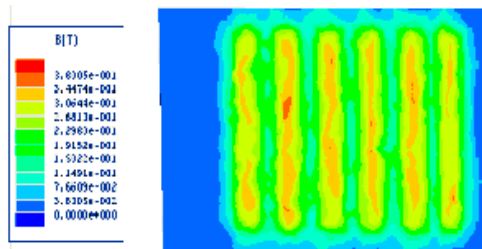


Figure (2) Flux density distribution when $v_r=0$ [7]

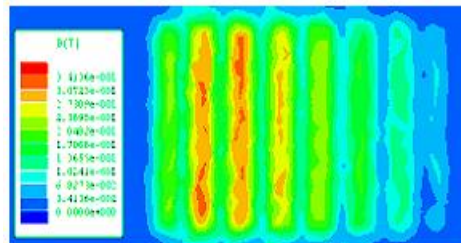


Figure (3) Flux density distribution when $v_r \neq 0$ [7]

Equivalent Circuit Models And Components

The approximate equivalent circuit of a LIM is presented in Figure 4. This circuit is on a per phase basis. Skin effect is small at rated frequency for a flat linear induction motor with a thin conductive sheet on the secondary. Therefore, equivalent secondary inductance is negligible [6]. The remaining non-negligible parameters are discussed as [8]:

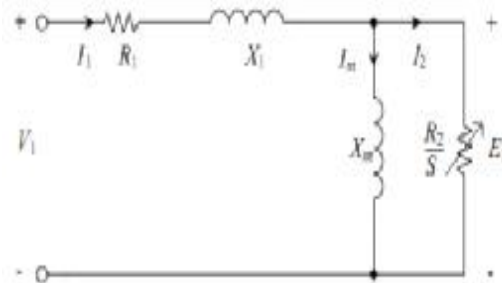


Figure (4) Per-phase SLIM equivalent circuit [9]

i) Per-phase stator resistance (R_1)

$$R_1 = \rho_w \frac{l_w}{A_w} \quad \dots (1)$$

Where, ρ_w is the volume resistivity of the copper wire used in the stator winding, l_w is the length of the copper wire per phase, and A_w is the cross-sectional area of the wire.

ii) Per-phase stator-slot leakage reactance X_1

$$X_1 = \frac{2\mu_0\pi f [(\lambda_s(1+\frac{3}{p})+\lambda_d)\frac{w_s}{q_1}+\lambda_e l_{ce}] N_1^2}{p} \quad \dots (2)$$

Where, f is the frequency, p number of poles, w_s slot width, q_1 number of slots/pole/phase in the stator, l_{ce} length of end connection, N_1 turns per phase

$$\lambda_s = \frac{h_s(1+3k_p)}{12w_s}$$

And;

$$\lambda_e = 0.3(3k_p - 1) \quad ,$$

and

$$\lambda_d = \frac{5(\frac{ge}{w_s})}{5+4(\frac{go}{w_s})}$$

iii) Per-phase magnetizing reactance (X_m)

$$X_m = \frac{24\mu_0\pi f W_{se} k_w N_1^2 \tau}{\pi^2 p g_e} \quad \dots (3)$$

Where, W_{se} is the equivalent stator width, τ pole pitch, k_w winding factor gain, g_e effective air-gap.

iv) Per-phase rotor resistance R_2

$$R_2 = \frac{X_m}{G} \dots\dots (4)$$

Where G is goodness factor

DESIGN AND OPTIMIZATION OF SLIM

Design of LIM model depends on the data which depend essentially on the topology of the motor such as stator width, air gap, motor slip, secondary thickness, power supply voltage and frequency.

The performance of the SLIM is evaluated by varying many design parameters like the thickness of secondary, mechanical air-gap and the number of poles of the reference model that shown in table 1. Each one of these parameters is varying many times to get the optimum value.

The analysis procedure is carried by varying one parameter of the reference model and keeps the others constants and then the effect of varying these parameters on the performance of SLIM are analyzed and the results are discussed.

The most important equations that used in design and optimization are the force, efficiency, and power factor as below [5]:

$$F_s = \frac{mI_1^2 R_2}{[(SG)^2] v_s S} \dots\dots(5)$$

$$\eta = \frac{F_s 2\tau f_1 (1-S)}{F_s 2\tau f_1 + 3R_1 I_1^2} \dots\dots(6)$$

$$\cos \phi = \frac{F_s 2\tau f_1 + 3R_1 I_1^2}{3V_1 I_1} \dots\dots (7)$$

The best optimized value, which gives the higher efficiency power factor product value is selected to give the final design of the modified proposed model.

OPTIMIZATION RESULTS

The optimization is carried by consider the first case by varying aluminum thickness of the secondary part and keep the other parameters constants, the effects of this parameter on SLIM performance are shown in Figure (5).

It is clear from the figure that increasing in AL thickness lead to decrease in efficiency P.F ($\eta \cos \phi$) product value.

Second case by varying air gap depth and keep the other parameters constants, the effect of this parameter on SLIM performance is shown in Figure (6).

It shows that increasing in air gap depth lead to decrease in efficiency P.F product value.

Third case by changing number of poles and keep the other parameters constants, the effect of this parameter on SLIM performance is shown in Figure (7).

In this case, increasing in number of poles lead to increasing in efficiency P.F product value.

Fourth case by changing slip and keep the other parameters constants, the effect of this parameter on SLIM performance is shown in Figure (8).

Hence increasing in slip lead to increasing in efficiency P.F product value.

OPTIMIZED MODEL

From the optimization results of the variation of efficiency P.F product with variation of speed as the criteria of the SLIM performance for different motor parameters changing, the modified model of SLIM can be selected with the aid of maximum efficiency P.F product for each case.

Figure (9) shows the improvement in the motor performance through the enhancement of the criteria factor at the rated speed 16 *m/sec*:

The efficiency P.F product value increases to 0.663 for model 2 while it is approximately 0.23 on model 1 for the same rated speed.

SIMULATION OF SLIM BY MATLAB/SIMULINK

The simulation of SLIM was performed using MATLAB/SIMULINK implementation program version 7.8 (R2009a). The proposed motor model was simulated in stationary reference frame, where the primary and secondary flux reference is along the d-q axes.

The block diagram of SLIM simulation based on MATLAB/SIMULINK is shown in Figure (10). On the scope, the result can be displayed with respect to simulation time. The input parameters and initial conditions to the system are defined by MATLAB M-file and initialized to the simulation steps.

Figure (11) shows speed variation with time. The speed ramp to rated speed within the first 20 *msec*. The end-effect factor $(1 - f(Q))$ is computed according to the speed value and introduced into the solution and its variation with time is shown in Figure (12). This factor starts from value 1 at the instant of starting and decrease to about 0.49 at 20 *msec*. The electromagnetic force (thrust force) variation with time is shown in Figure (13).

CONCLUSIONS

The reduction in the aluminum thickness leads to an increase in the efficiency and power factor value.

Also, the decreasing the air-gap leads to an increasing in the efficiency and power factor values, hence increasing their product.

The increasing of number of poles leads to an increasing in efficiency power factor product value.

And, increasing of the secondary slip lead to an increasing of power factor, while a small reduction in the efficiency but as a result the efficiency power factor product value increases.

REFERENCES

- [1]. I. Boldea, and S. A. I. Nasar " The Induction Machine Handbook " CRC press LLC, 2002.
- [2]. Bonneya, M. F. " Modeling and Optimization of Linear Induction Motor Using Finite Element Method ", Ph.D thesis, University of Technology, Baghdad, Iraq, 2009.
- [3]. Byung-jun Lee, Dae-hyun Koo and Yun-hyun Cho," Investigation of Secondary Conductor Type of Linear Induction Motor Using the Finite Element Method", IEE Proc.-Electr. Power Appl., 2008.
- [4]. Hassanpour Isfahani,A. B. M. Ebrahimi, and H. Lesani" Design Optimization of a Low-Speed Single-Sided Linear Induction Motor for Improved Efficiency and Power Factor" IEEE transactions on magnetics, Vol. 44, No. 2, February, 2008.
- [5]. Duncan, J. "Linear Induction Motor Equivalent Circuit Model" IEE Proc, Vol. 130,Pt. B, No.1, January 1983.
- [6]- Adil H. Ahmad and Mehdi F. Bonneya" Finite Element Analysis of Single Sided Linear Induction Motor" accepted at Engineering and Technology Journal /UOT/ Baghdad No. 821, 7/4/2010.
- [7].Gang, LV LIQiang, LIU Zhiming, FAN Yu and LI Guo-guo, "The Analytical Calculation of the Thrust and Normal Force and Force Analyses for Linear Induction Motor" ICSP2008 Proceedings, 2008.
- [8]. Sarveswara Bhamidi," Design of a Single Sided Linear Induction Motor (SLIM) using a user Interactive Computer Program ", M.Sc. thesis, University of Missouri-Columbia, 2005.
- [9]. Zuorong Zhang, Tony R. Eastham and Graham E. Dawson" LIM Dynamic Performance Assessment from Parameter Identification" Proceeding of IEEE conference ,pp. 295-300, vol.1, Toronto, Canada, 1993.

Table (1) gives the main parameters of the reference model [5].

<i>Item No.</i>	<i>Parameter name</i>	<i>Symbol</i>	<i>Unit</i>	<i>Parameter value</i>
1	<i>Force (thrust)</i>	F_s	<i>N</i>	8611
2	<i>Secondary thickness</i>	d	<i>m</i>	0.003
3	<i>Physical air-gap</i>	g_m	<i>m</i>	0.01
4	<i>No. of poles</i>	p	-	4
5	<i>Operating slip</i>	S	-	10%
6	<i>No. of slot/pole/phase</i>	q_1	-	1
7	<i>Supply voltage</i>	V_s	<i>volt</i>	380 l.l
8	<i>Supply frequency</i>	f_s	<i>Hz</i>	50
9	<i>Stator width</i>	w_s	<i>mm</i>	3.14
10	<i>Rated speed</i>	v_r	<i>m/sec</i>	16

Table (2) shows the main parameters of the modified model.

Item no.	Parameter name	Symbol	Unit	Parameter value
1	Force (thrust)	F_s	N	8611
2	Secondary thickness	d	m	0.001
3	Physical air-gap	g_m	m	0.005
4	Total gap	g_0	m	0.006
5	No. of poles	p	-	8
6	Operating slip	S	-	3%
7	No. of slot/pole/phase	q_1	-	1
8	Efficiency	η	-	0.8095
9	Power factor	pf	-	0.820
10	Efficiency * P.F	$\eta \cos \varphi$	-	0.663
11	Primary resistance	R_1	Ω	0.0419
12	Secondary resistance	R_2	Ω	0.1306
13	Primary reactance	X_1	Ω	0.2559
14	Magnetizing reactance	X_m	Ω	2.51
15	Total impedance	Z	Ω	$0.4646+j0.3292$
16	Input power	P_{in}	watt	650

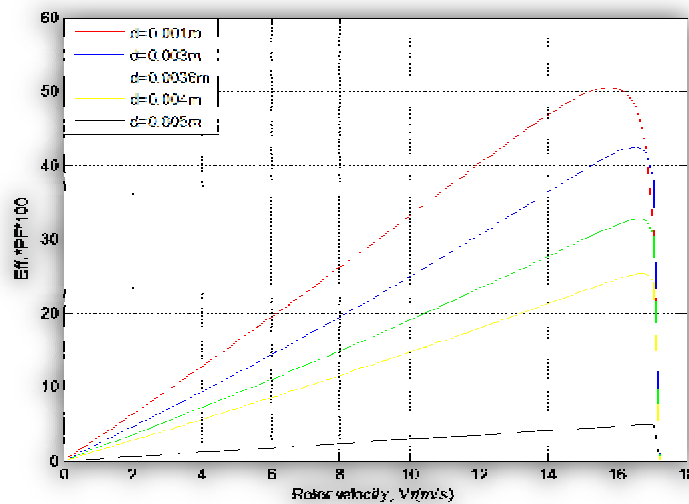


Figure (5) Variation of $\eta \cos \varphi$ product with speed for different AL thickness.

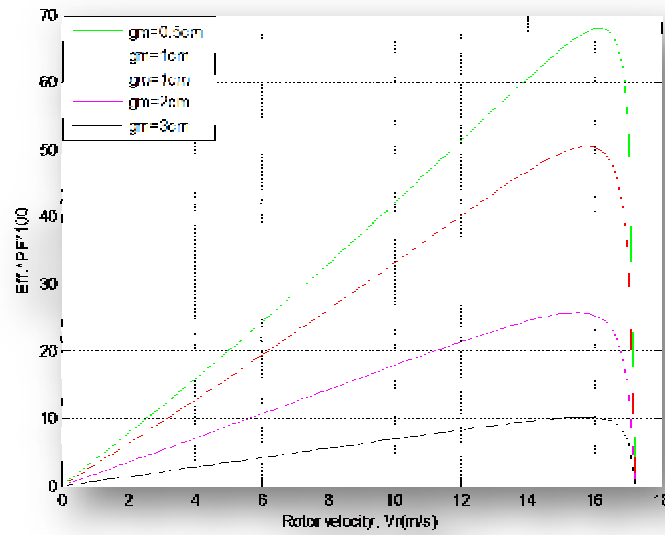


Figure (6) Variation of $\eta \cos \phi$ product with speed for different air gap depths.

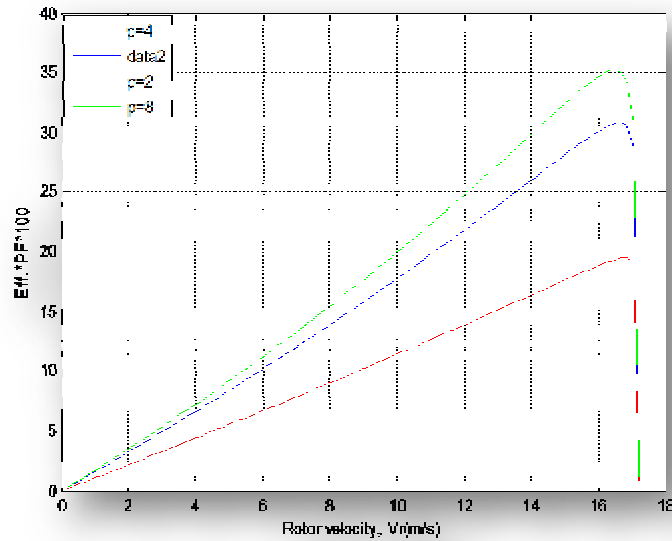


Figure (7) Variation of $\eta \cos \phi$ product with speed for different number of poles.

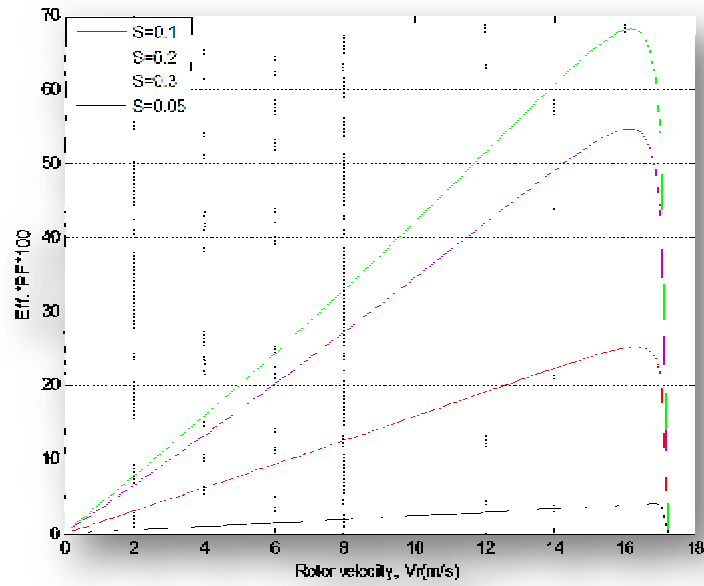


Figure (8) Variation of $\eta \cos \phi$ product with speed with changing slip.

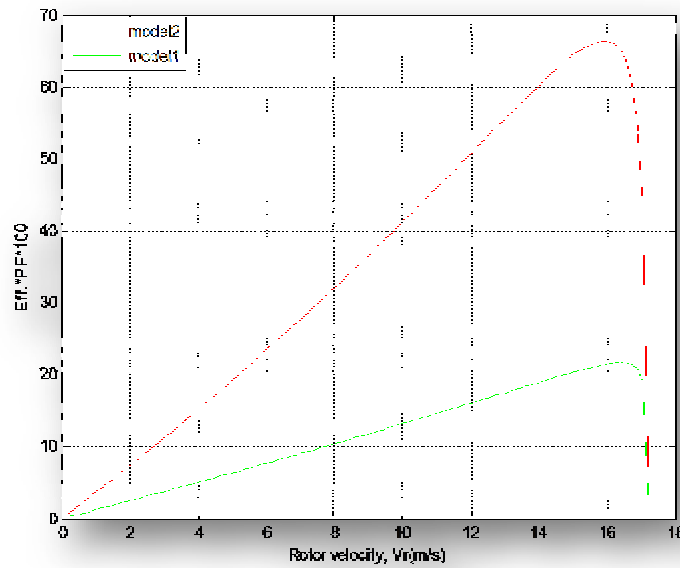


Figure (9) A comparison between the two models based on the $\eta \cos \phi$ product criteria.

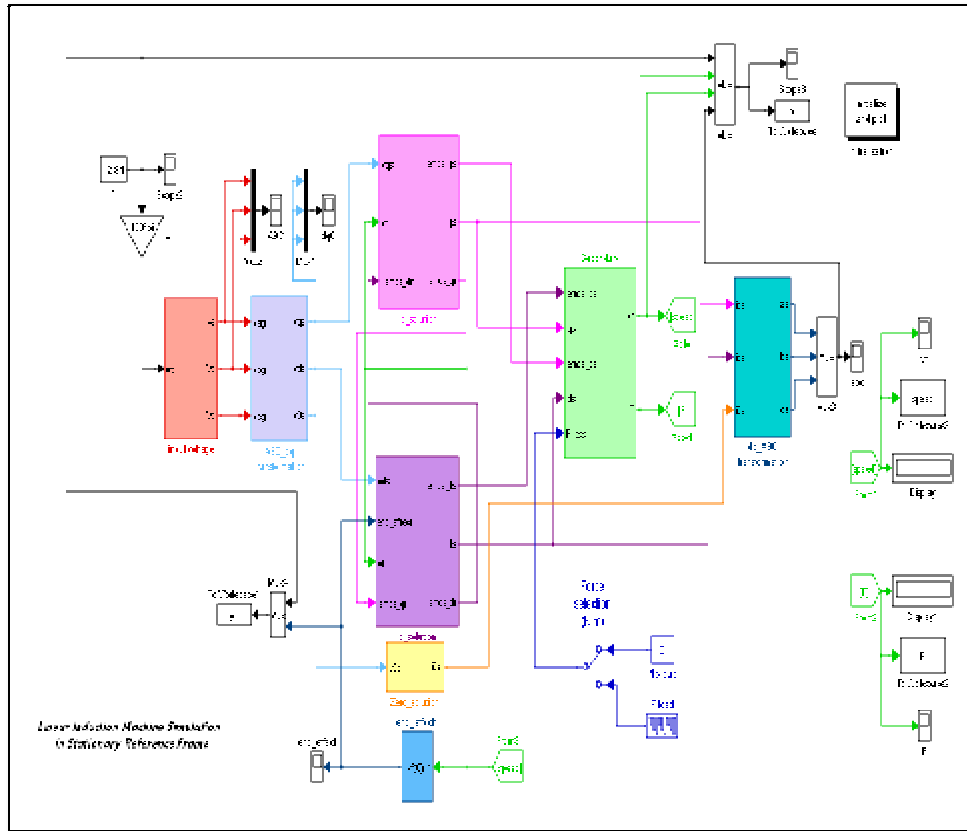


Figure (10) SLIM simulation using stationary reference frame in MATLAB/SIMULINK

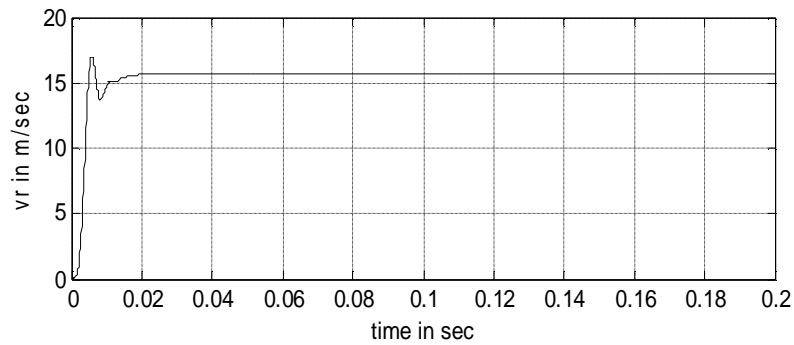


Figure (11) Speed variation with time.

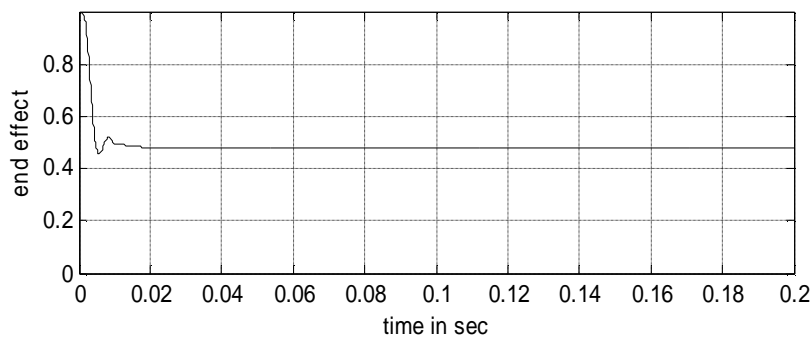


Figure (12) End-effect factor ($1 - f(Q)$) variation with time.

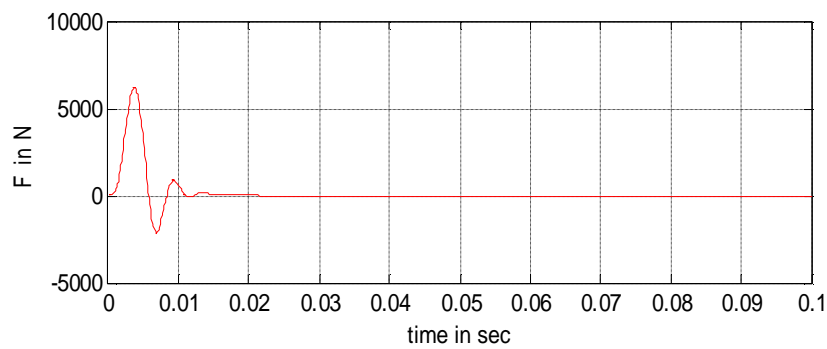


Figure (13) The electromagnetic force (thrust force) generated for SLIM.